

# Thermodynamic Evidence for Negative Charge Stabilization by a Catalytic Metal Ion within an RNA Active Site

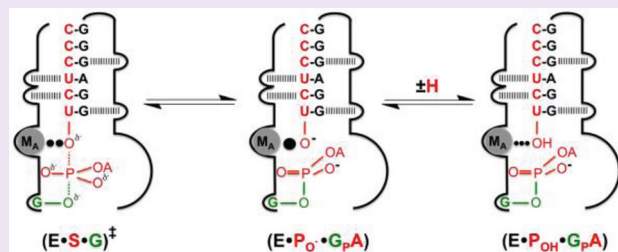
Raghuvir N. Sengupta,<sup>†,‡</sup> Daniel Herschlag,<sup>‡,\*</sup> and Joseph A. Piccirilli<sup>†,\*</sup>

<sup>†</sup>Department of Biochemistry & Molecular Biology and Department of Chemistry, The University of Chicago, 929 East 57th Street, Gordon Center for Integrative Science W406, Chicago, Illinois 60637, United States

<sup>‡</sup>Department of Biochemistry, Stanford University, Beckman Center, B400, Stanford, California 94305-5307, United States

## Supporting Information

**ABSTRACT:** Protein and RNA enzymes that catalyze phosphoryl transfer reactions frequently contain active site metal ions that interact with the nucleophile and leaving group. Mechanistic models generally hinge upon the assumption that the metal ions stabilize negative charge buildup along the reaction coordinate. However, experimental data that test this assumption directly remain difficult to acquire. We have used an RNA substrate bearing a 3'-thiol group to investigate the energetics of a metal ion interaction directly relevant to transition state stabilization in the *Tetrahymena* group I ribozyme reaction. Our results show that this interaction lowers the  $pK_a$  of the 3'-thiol by 2.6 units, stabilizing the bound 3'-thiolate by 3.6 kcal/mol. These data, combined with prior studies, provide strong evidence that this metal ion interaction facilitates the forward reaction by stabilization of negative charge buildup on the leaving group 3'-oxygen and facilitates the reverse reaction by deprotonation and activation of the nucleophilic 3'-hydroxyl group.



Phosphoryl transfer reactions are central to the performance and regulation of essentially every cellular process, and many protein and RNA enzymes mediating these reactions employ metal ions in catalysis. In their classic review, Benkovic and Schray envisaged a number of roles for catalytic metal ions in biological phosphoryl transfer, including (a) serving as a template for organizing the active site and orienting substrates and (b) neutralizing negative charge buildup.<sup>1</sup> Supported by precedent established through analysis of well-defined model systems, these catalytic modes implicitly underlie most models for metalloenzyme-catalyzed phosphoryl transfer.<sup>2–4</sup> The templating mode follows logically from ground state metal ion interactions with substrates and chelating ligands, usually inferred from structural inspection and spectroscopy.<sup>2,4</sup> However, negative charge frequently borne by the chelating ligands (e.g., anionic side chains in proteins and phosphate oxygen atoms in RNA) that mediate these ground state interactions may attenuate the electropositive potential of the active site metal ions and thereby render the catalytic contribution of charge neutralization in the transition state ambiguous. Moreover, assessing the ability of active site metal ions to neutralize negative charge poses significant experimental challenges, and there exist limited data that support this mode of metal ion catalysis directly (e.g., see ref 5).

Metal ions at the active site of the *Tetrahymena* ribozyme were initially revealed from metal ion rescue experiments that take advantage of the preference for interactions of soft metal ions with sulfur and nitrogen relative to oxygen.<sup>6</sup> Early functional work identified metal ion interactions in the

transition state involving the guanosine 3'-oxygen nucleophile and the adjacent 2'-hydroxyl group, the U(-1) 3'-oxygen leaving group, and a nonbridging oxygen atom of the transferred phosphoryl group (Figure 1). Thereafter, applica-

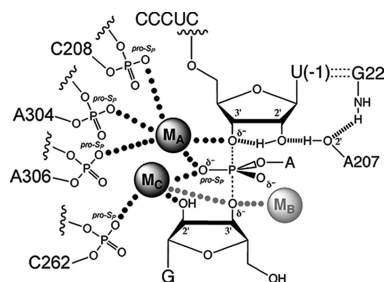


**Figure 1.** Model of the transition state of the group I self-splicing reaction from functional and structural data.<sup>6</sup> Dotted and hatched lines denote metal ion interactions and hydrogen bonds, respectively. Metal ion interactions supported by functional and structural evidence are colored black. Functional data suggest that the 3'-oxygen atom of G interacts with a metal ion ( $M_B$ , shown in gray) distinct from  $M_C$ . The structural data provide no evidence for  $M_B$  and suggest that the 3'-oxygen atom of G coordinates to  $M_C$  (represented by gray dots), the same metal ion that interacts with the 2'-OH group of G.

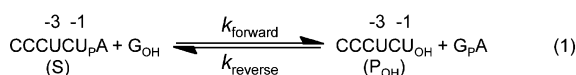
Received: June 22, 2011

Accepted: October 27, 2011

Published: October 27, 2011

tion of a quantitative approach termed Thermodynamic Fingerprint Analysis (TFA) provided information about the affinity of the rescuing metal ions and ascribed the identified interactions to three distinct metal ions:  $M_A$ ,  $M_B$ , and  $M_C$  (Figure 1).<sup>7</sup> Subsequent X-ray analysis of crystals derived from the *Azoarcus* group I intron revealed the locations of two metal ions, corresponding to  $M_A$  and  $M_C$ , within the active site.<sup>8</sup> In the structure-derived model,  $M_C$  supplants the role of the missing metal ion ( $M_B$ ). This unresolved difference may reflect limitations in either the functional or structural results or possibly idiosyncratic differences associated with distinct evolutionary subclasses of introns.<sup>6</sup>

The structural and functional data for  $M_A$  show perfect agreement, and in this work we investigate an important and potentially general mechanistic role for this metal ion (Figure 1).  $M_A$  contacts the U(-1) 3'-oxygen atom, which is the leaving group in the forward reaction and the nucleophile in the reverse reaction (eq 1). Mechanistic models inferred from this contact



implicitly assume that  $M_A$  imparts catalysis *via* electrostatic charge neutralization, stabilizing the negative charge that develops on the leaving group en route to the transition state and activating the nucleophile by increasing the amount of the corresponding anion. Nevertheless,  $M_A$  ranks among the mostly highly chelated metal ions observed in an RNA structure, with three negatively charged phosphate ligands from the catalytic core (C208, A304, and A306) making direct inner sphere coordination (Figure 1).<sup>8,9</sup> To assess whether  $M_A$  can function in leaving group stabilization and nucleophile activation, we have used an extension of TFA to evaluate its capacity for electrostatic stabilization within the active site.

We first tested whether a metal ion forms a ground state contact with the U(-1) 3'-OH group of  $P_{\text{OH}}$  by using two analogues containing in place of the 3'-OH group either a thiol group (-SH, herein referred to as " $P_{\text{SH}}$ ") or a hydrogen atom (-H, herein referred to as " $P_{\text{H}}$ "). Neither of these oligonucleotides serves as a substrate for the reverse reaction (eq 1,  $k_{\text{reverse}}$ ),  $P_{\text{H}}$  because it lacks a nucleophile and  $P_{\text{SH}}$  because sulfur has extremely low nucleophilicity toward phosphorus.<sup>10</sup> To characterize these substrates, we took advantage of a previously studied miscleavage reaction that is catalyzed by the ribozyme and  $G_{\text{OH}}$  in the absence of added  $G_P\text{A}$ . We were able to use this ribozyme-catalyzed miscleavage reaction to obtain a readout of active site binding strength and interactions, as illustrated in Figure 2A and described below.

$P_{\text{OH}}$  binds to the *Tetrahymena* ribozyme (E) in two distinct steps:  $P_{\text{OH}}$  first makes base-pairing interactions with the internal guide sequence of E to form the "open" ( $E \cdot P_{\text{OH}}$ )<sub>O</sub> complex, and the resulting P1 duplex then docks *via* tertiary interactions into the catalytic core of the ribozyme to form the "closed" ( $E \cdot P_{\text{OH}}$ )<sub>C</sub> complex (Figure 2a).<sup>6</sup> Binding of  $G_{\text{OH}}$  to the ( $E \cdot P_{\text{OH}}$ )<sub>C</sub> complex does not lead to a cleavage product directly, but the P1 duplex can undock from the ( $E \cdot P_{\text{OH}}$ )<sub>C</sub> complex and redock transiently in a different, less stable register to form a misdocked complex, ( $E \cdot P_{\text{OH}}$ )<sub>C'</sub> (Figure 2a).<sup>11</sup> In a misdocked complex, the P1 duplex is displaced by one or more base pairs with respect to the tertiary interactions, placing a different base pair at the active site, thereby leading to aberrant cleavage by  $G_{\text{OH}}$ , most prominently at the U(-3) position of  $P_{\text{OH}}$  (Figure 2a).<sup>11,12</sup>

In 10 mM  $\text{Mg}^{2+}$ , where all catalytic metal sites (Figure 1) are occupied by  $\text{Mg}^{2+}$ ,<sup>13</sup>  $P_{\text{H}}$  and  $P_{\text{SH}}$  undergo miscleavage by  $G_{\text{OH}}$  at similar rates, approximately 50- and 75-fold faster than the rate of  $P_{\text{OH}}$  miscleavage, respectively (Figure 2b, black bars). According to the model illustrated in Figure 2a, the faster miscleavage of  $P_{\text{H}}$  and  $P_{\text{SH}}$  results from an increase in the fraction of time in which the ( $E \cdot P_X$ ) complex is in the misdocked state. Higher occupancy of the misdocked state by  $P_{\text{H}}$  and  $P_{\text{SH}}$  relative to  $P_{\text{OH}}$  indicates a decrease in stability of the correctly docked ( $E \cdot P_{\text{H}}$ )<sub>C</sub> and ( $E \cdot P_{\text{SH}}$ )<sub>C</sub> complexes relative to the ( $E \cdot P_{\text{OH}}$ )<sub>C</sub> complex.<sup>11</sup> This difference in stability with the different versions of P presumably reflects the presence of a favorable interaction with the 3'-OH that stabilizes the ( $E \cdot P_{\text{OH}}$ )<sub>C</sub> binding mode but is weakened or absent in the ( $E \cdot P_{\text{H}}$ )<sub>C</sub> and ( $E \cdot P_{\text{SH}}$ )<sub>C</sub> complexes due to the absence of the 3'-OH group. The decrease in the stability of the ( $E \cdot P$ )<sub>C</sub> complex shifts the docking equilibrium toward ( $E \cdot P$ )<sub>O</sub> (see below), which allows the  $P_{\text{SH}}$  and  $P_{\text{H}}$  substrates to sample the alternative misdocked ( $E \cdot P$ )<sub>C'</sub> binding mode more frequently, resulting in faster miscleavage in the presence of  $G_{\text{OH}}$ .

Considering that the U(-1) 3'-oxygen interacts with  $M_A$  in the transition state (Figure 1), destabilization of the ( $E \cdot P_X$ )<sub>C</sub> binding mode by  $P_{\text{H}}$  or  $P_{\text{SH}}$  could reflect disruption of the interaction between the 3'-OH and this active site metal ion in the ground state:  $P_{\text{H}}$  lacks a ligand altogether and sulfur coordinates much more weakly to  $\text{Mg}^{2+}$  than oxygen does.<sup>14</sup> To test the possibility that the 3'-OH interacts with a metal ion in the ground state ( $E \cdot P_{\text{OH}}$ )<sub>C</sub> complex, we monitored miscleavage of  $P_{\text{OH}}$ ,  $P_{\text{H}}$ , and  $P_{\text{SH}}$  in the presence of 1 mM  $\text{Mn}^{2+}$ .  $\text{Mn}^{2+}$  decreased the rate of miscleavage of  $P_{\text{SH}}$  but did not affect the miscleavage rates for  $P_{\text{OH}}$  or  $P_{\text{H}}$  (Figure 2b, gray bars). We attribute the specific inhibition of  $P_{\text{SH}}$  miscleavage by  $\text{Mn}^{2+}$  to stabilization of the ( $E \cdot P_{\text{SH}}$ )<sub>C</sub> complex. As  $\text{Mn}^{2+}$  coordinates sulfur more strongly than  $\text{Mg}^{2+}$  does,<sup>14</sup> stabilization of the ( $E \cdot P_{\text{SH}}$ )<sub>C</sub> complex by  $\text{Mn}^{2+}$  provides strong evidence that  $\text{Mn}^{2+}$  interacts with the U(-1) 3'-sulfur in the ( $E \cdot P_{\text{SH}}$ )<sub>C</sub> complex.

To further explore the  $\text{Mn}^{2+}$  stabilization of correct docking that we observed by following  $P_{\text{SH}}$  miscleavage, we directly determined dissociation rate constants ( $k_{\text{off}}$ ) for  $P_{\text{SH}}$  as a function of  $\text{Mn}^{2+}$  concentration in a 10 mM  $\text{Mg}^{2+}$  background using pulse-chase methods. In the absence of  $\text{Mn}^{2+}$ ,  $P_{\text{SH}}$  and  $P_{\text{H}}$  dissociate from the ribozyme approximately 20- to 30-fold faster than does  $P_{\text{OH}}$  (Figure 2c and Supplementary Table S1), consistent with the 50- to 75-fold greater miscleavage rates observed (Figure 2b) and with previous results for  $P_{\text{H}}$ .<sup>15</sup> Addition of  $\text{Mn}^{2+}$  reduced  $k_{\text{off}}$  for  $P_{\text{SH}}$  by approximately 200-fold, whereas the effect of  $\text{Mn}^{2+}$  on  $P_{\text{OH}}$  and  $P_{\text{H}}$  dissociation was  $\leq 2$ -fold (Supplementary Table S1). The observed decrease in  $P_{\text{SH}}$  dissociation by  $\text{Mn}^{2+}$  provides additional support for the model in which a metal ion interacts with the U(-1) 3'-SH to stabilize correct docking of the ( $E \cdot P_{\text{SH}}$ ) complex. We infer that a metal ion interacts with U(-1) 3'-OH analogously to stabilize correct docking of  $P_{\text{OH}}$ .

We used TFA to assess whether  $M_A$  mediates the stabilizing interaction in the closed complex. The  $\text{Mn}^{2+}$  concentration dependence of  $k_{\text{off}}$  for  $P_{\text{SH}}$  dissociation allowed us to determine the apparent affinity of the  $\text{Mn}^{2+}$  that stabilizes the ( $E \cdot P_{\text{SH}}$ )<sub>C</sub> complex ( $K_{(\text{E} \cdot \text{P}_{\text{SH}})}^{\text{Mn,app}} = 3.2 \pm 0.6 \mu\text{M}$ , Figure 2c). With this measurement, we could use the thermodynamic cycle shown in Figure 2d to calculate the apparent affinity of this  $\text{Mn}^{2+}$  for binding to E in the absence of the -SH ligand ( $K_{(\text{E})}^{\text{Mn,app}} = 0.58 \pm 0.1 \text{ mM}$ ). This value is consistent with the apparent affinity of  $\text{Mn}^{2+}$  for binding to the  $M_A$  site in the ribozyme in the absence

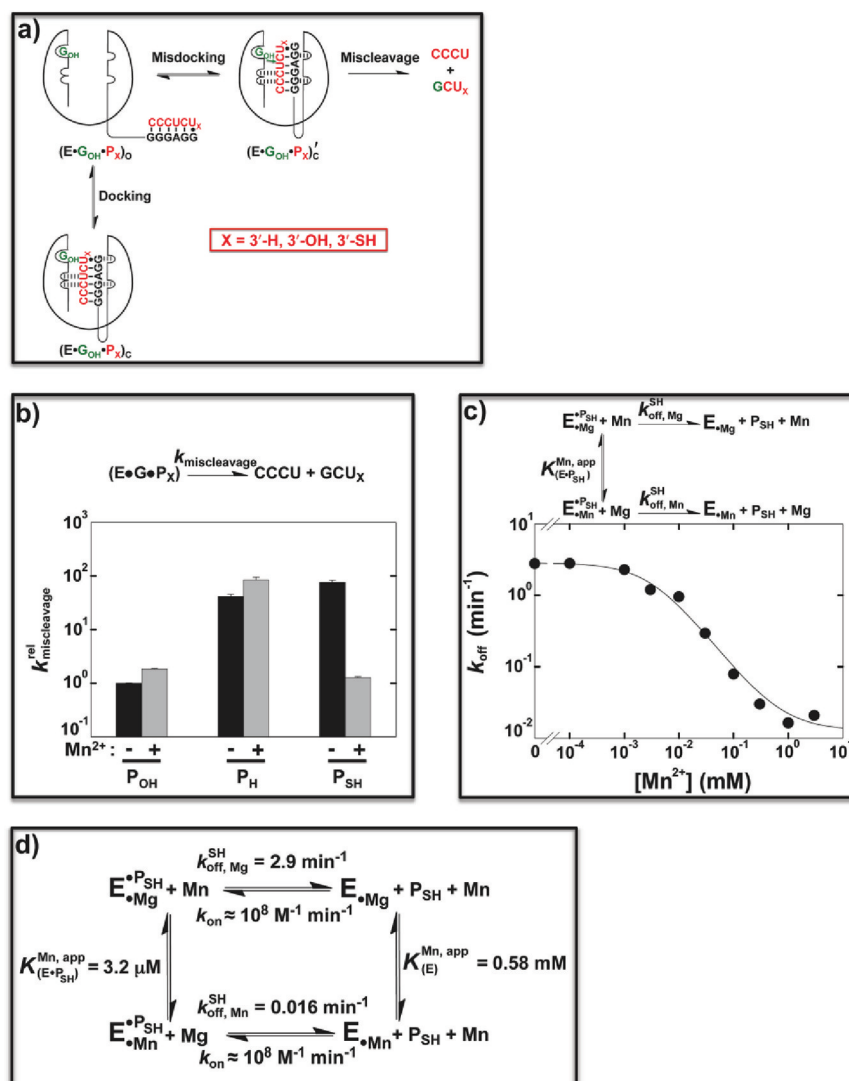


**Figure 2.**  $M_A$  facilitates proper docking of the (E·P) complex. (a) The ribozyme-catalyzed miscleavage reaction. Hatched lines denote tertiary contacts between the ribozyme and 2'-OH groups on P<sub>X</sub>. The green arrow indicates nucleophilic attack by the 3'-OH of G. (b) Miscleavage rate constants for P<sub>H</sub>, P<sub>OH</sub>, and P<sub>SH</sub> in the absence (black) and presence (gray) of 1 mM MnCl<sub>2</sub>.  $k_{\text{miscleavage}}^{\text{rel}}$  is the rate constant for miscleavage of P<sub>X</sub> with or without Mn<sup>2+</sup> present relative to the P<sub>OH</sub> miscleavage rate constant in the absence of Mn<sup>2+</sup>. (c) Plot of  $k_{\text{off}}$  vs [Mn<sup>2+</sup>] for P<sub>SH</sub>. The line is a fit of the data to binding of a single Mn<sup>2+</sup> ion and gives an apparent Mn<sup>2+</sup> affinity ( $K_{(\text{E} \cdot \text{P}_{\text{SH}})}^{\text{Mn, app}}$ ) of  $3.2 \pm 0.6 \mu\text{M}$ . (d) Thermodynamic cycle showing coupling between P<sub>SH</sub> and Mn<sup>2+</sup> binding to metal site A.  $k_{\text{off, Mg}}^{\text{SH}}$ ,  $k_{\text{off, Mn}}^{\text{SH}}$ , and  $K_{(\text{E} \cdot \text{P}_{\text{SH}})}^{\text{Mn, app}}$  were obtained from the data in Figure 2c.  $K_{(\text{E})}^{\text{Mn, app}}$  was calculated from the thermodynamic cycle shown in this panel. An association rate constant ( $k_{\text{on}}$ ) of  $10^8 \text{ M}^{-1} \text{ min}^{-1}$  was assumed for P<sub>SH</sub> (Supplementary Table S2).<sup>13</sup>

of bound substrate, obtained from independent experiments using substrate cleavage assays as described previously (R.N.S, J.A.P., and D.H., unpublished data).<sup>7</sup> This agreement suggests that the metal ion that stabilizes docking of P in the ground state also provides stabilizing interactions to the U(-1) 3'-oxygen atom in the transition state (*i.e.*,  $M_A$ , Figure 1).<sup>7</sup> These results, in conjunction with prior structural and functional data,<sup>9</sup> link  $M_A$  to ground and transition state interactions with the U(-1) 3'-oxygen atom.

Interactions with  $M_A$  may stabilize the negative charge that builds up on the leaving group and nucleophile as they traverse the reaction coordinate in the forward and reverse directions, respectively. However, such stabilization for formation of an oxyanion from a hydroxyl group frequently eludes direct measurement because RNA's 3'-hydroxyl group ( $\text{p}K_a \sim 13$ ) generally ionizes at pH values higher than the range observable for a biomolecule.<sup>16</sup> Moreover, ribozymes can exhibit complex

pH-rate profiles, rendering it difficult to ascribe  $\text{p}K_a$  values to specific functional groups.<sup>6</sup> In contrast, thiols generally ionize with  $\text{p}K_a$  values significantly lower than the corresponding alcohols,<sup>17</sup> raising the possibility that substitution of the hydroxyl group with a thiol could lower the  $\text{p}K_a$  of the enzyme-bound species to within an observable range.

To probe the electrostatic character of  $M_A$  in the context of its RNA active site, we assessed whether binding of P<sub>SH</sub> to the ribozyme affects the  $\text{p}K_a$  of the U(-1) 3'-SH. First, we measured the solution  $\text{p}K_a$  of the P<sub>SH</sub> thiol by monitoring alkylation by iodoacetamide,<sup>18</sup> which reacts with the thiolate anion significantly faster than with the neutral thiol (Figure 3a). The pH-dependence of P<sub>SH</sub> alkylation gave a solution  $\text{p}K_a$  of  $7.6 \pm 0.1$  (Figure 3a,  $\text{p}K_a^{\text{P}_{\text{SH}}}$ ). Next, we measured  $k_{\text{off}}$  for dissociation of P<sub>SH</sub> from the ribozyme as a function of pH. With Mg<sup>2+</sup> as the only divalent cation present, P<sub>SH</sub> dissociated from the ribozyme with a rate constant of approximately 3 min<sup>-1</sup>

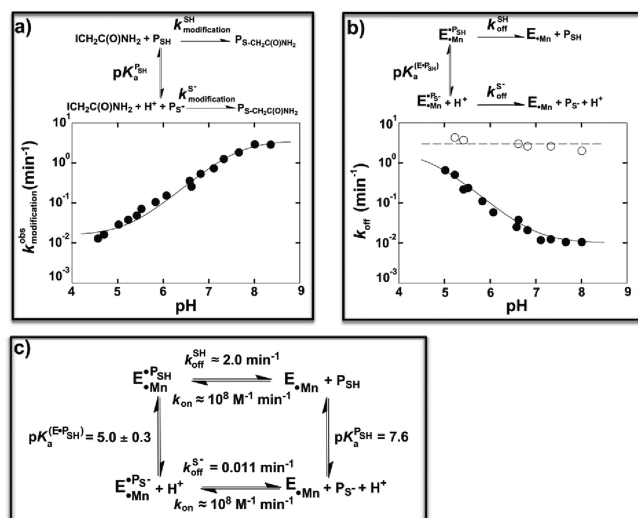


**Figure 3.**  $M_A$  lowers the  $pK_a$  of the U(-1) 3'-SH group. a) Iodoacetamide modification of  $P_{SH}$  in solution as a function of pH. The line is a fit of the data to ionization of the -SH group and gives an apparent  $pK_a$  value ( $pK_a^{P_{SH}}$ ) of  $7.6 \pm 0.1$ . b) Dissociation rate constant of  $P_{SH}$  as a function of pH in the absence (open circles) and presence (closed circles) of 1 mM  $Mn^{2+}$ . The dashed line passing through the open circles is a straight line, with  $k_{off}$  set to  $3 \text{ min}^{-1}$ . The line passing through the closed circles is a fit of the data to ionization of the -SH group in the  $(E \cdot P_{SH})$  complex assuming a value of  $2 \text{ min}^{-1}$  for  $k_{off}^{SH}$ , as described in the text. This fit gives a value of  $pK_a^{(E \cdot P_{SH})} = 4.7 \pm 0.3$ . c) Thermodynamic cycle showing coupling between  $P_{SH}$  binding and ionization of the -SH group.  $pK_a^{P_{SH}}$  was obtained from the data in Figure 3a.  $k_{off}^{SH}$  was approximated as described in the text.  $k_{off}^{S^-}$  was obtained from  $k_{off}$  for  $P_{SH}$  in the presence of  $Mn^{2+}$  at high pH, as shown in Figure 3b. An association rate constant ( $k_{on}$ ) of  $10^8 \text{ M}^{-1} \text{ min}^{-1}$  was assumed (Table S2).<sup>13</sup>  $pK_a^{(E \cdot P_{SH})} = 5.0 \pm 0.3$  reflects the average of  $pK_a^{(E \cdot P_{SH})} = 5.3$  calculated from the thermodynamic cycle and  $pK_a^{(E \cdot P_{SH})} = 4.7$  determined from the fit of the data shown in Figure 3b.

from pH 5 to 8 (Figure 3b, open circles). This  $k_{off}$  value matches measurements for other substrates that primarily populate the open complex (Figure 2a).<sup>12,19</sup> This agreement and the  $P_{SH}$  miscleavage data presented above suggest that the  $(E \cdot P_{SH})$  complex exists predominantly in the open complex (Figure 2a), so that there is little or no direct interaction between the sulfur atom of  $P_{SH}$  and the  $Mg^{2+}$  ion that occupies site  $M_A$ . The pH-independence of dissociation indicates that binding in the open complex does not shift the  $pK_a$  of  $P_{SH}$  from its solution value. In contrast, when  $Mn^{2+}$  occupies the  $M_A$  site, increasing the pH from 5 to 8 decreases  $k_{off}$  for  $P_{SH}$  by 60-fold (Figure 3b, closed circles), whereas pH exerts little influence on dissociation of  $P_{OH}$  or  $P_H$  from the ribozyme ( $<4$ -fold; Supplementary Table S1). The pH-dependent decrease in  $k_{off}$  for  $P_{SH}$  conferred by  $Mn^{2+}$  can be explained if -SH ionizes to  $-S^-$  over this pH range and if  $Mn^{2+}$  forms a more favorable interaction with the thiolate anion  $-S^-$  than with the neutral thiol -SH. As described below, under this assumption, the pH-dependence of  $k_{off}$  allows measurement of the  $pK_a$  for  $P_{SH}$  in the  $(E \cdot P_{SH})$  complex in the presence of  $Mn^{2+}$ .

If  $Mn_A$  interacts more strongly with  $-S^-$  than with -SH, then according to the thermodynamic cycle shown in Figure 3c the ribozyme must lower the  $pK_a$  of the U(-1) 3'-SH. Using this cycle, we can estimate the  $pK_a$  of the U(-1) 3'-SH in the  $(E \cdot P_{SH})$  complex with knowledge of three equilibrium values: the solution  $pK_a$  of  $P_{SH}$  and the equilibrium constants for dissociation of  $P_{SH}$  and  $P_{S^-}$  from the ribozyme. The limiting value for dissociation of  $P_{SH}$  at high pH gives  $k_{off} = 0.011 \text{ min}^{-1}$  for the anionic ( $-S^-$ ) form of  $P_{SH}$  (Figure 3b,c). In contrast, we could not obtain  $k_{off}$  for the neutral (-SH) form of  $P_{SH}$  from the pH dependence due to the lack of a plateau in the low pH regime (Figure 3b). Additionally, complications associated with ribozyme inactivation prevented  $k_{off}$  measurements below pH 5. Instead, we estimated the dissociation rate constant for  $P_{SH}$  as follows. Fits of the reaction-rate profile at low pH give  $k_{off} > 1$

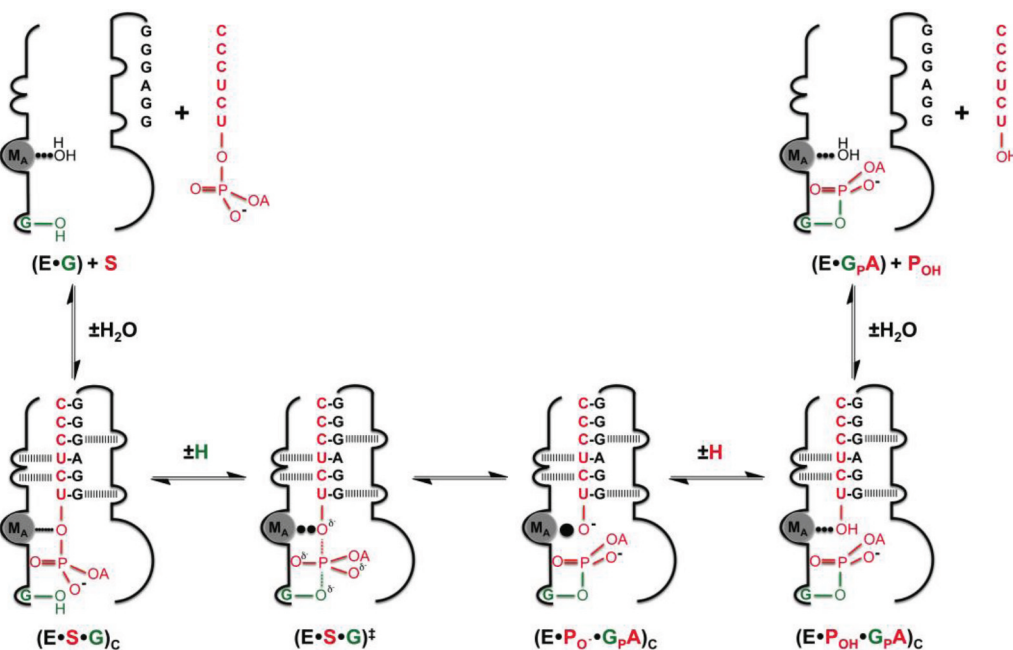


**Figure 4.** Model for the interaction between  $M_A$  and the U(-1) 3'-oxygen atom along the reaction cycle from the results of this study and previous work.<sup>15</sup> Dotted and hatched lines denote metal ion coordination and tertiary interactions, respectively. The size of the dots represents the extent of favorable electrostatic interaction between  $M_A$  and the U(-1) 3'-oxygen atom.

$\text{min}^{-1}$  as a lower limit for the value (Figure 3b, closed circles), and  $k_{\text{off}} = 3 \text{ min}^{-1}$ , the pH-independent rate constant for dissociation of  $\text{P}_{\text{SH}}$  in  $\text{Mg}^{2+}$  alone, provides an upper limit for this dissociation constant (Figure 3b, open circles). As these limits are similar, their average of  $2 \text{ min}^{-1}$  likely represents a reliable approximation for the dissociation rate constant of the neutral form of  $\text{P}_{\text{SH}}$  from the ribozyme.

In contrast to the large difference in  $k_{\text{off}}$  for the neutral and anionic forms of  $\text{P}_{\text{SH}}$ , both forms bind to the ribozyme with similar association rate constants ( $k_{\text{on}}$ , Supplementary Table S2). Continuing with the thermodynamic analysis in Figure 3c, our values of  $k_{\text{on}}$  and  $k_{\text{off}}$ , together with the  $\text{P}_{\text{SH}}$  solution  $\text{p}K_{\text{a}}$ , give three equilibrium constants in the cycle and allow calculation of the  $\text{p}K_{\text{a}}$  for bound  $\text{P}_{\text{SH}}$  as 5.3 ( $\text{p}K_{\text{a}}^{\text{(E-P}_{\text{SH}})}$ , Figure 3c). This value is similar to the  $\text{p}K_{\text{a}}$  of  $4.7 \pm 0.3$  obtained from the fit of the data in Figure 3b (closed circles), assuming a dissociation rate constant of  $2 \text{ min}^{-1}$  for the -SH form of  $\text{P}_{\text{SH}}$ . Taking the average of  $\text{p}K_{\text{a}}^{\text{(E-P}_{\text{SH}})}$  obtained from the fit (4.7) and from the thermodynamic cycle (5.3), we estimate an apparent  $\text{p}K_{\text{a}}$  of  $5.0 \pm 0.3$  for  $\text{P}_{\text{SH}}$  in the (E- $\text{P}_{\text{SH}}$ ) complex (Figure 3c). We thus conclude that  $\text{Mn}^{2+}$ -induced docking of  $\text{P}_{\text{SH}}$  into the ribozyme active site allows the electropositive character of the active site to manifest as a  $\text{p}K_{\text{a}}$  lowering of the U(-1) 3'-SH group by approximately 2.6 units, corresponding to stabilization of the thiolate anion by 400-fold or 3.6 kcal/mol.

Our analysis shows that  $M_{\text{A}}$ , although highly chelated by anionic active site phosphoryl oxygen atoms (Figure 1), retains sufficient electropositive character to mediate a stabilizing interaction with the thiolate anion. These findings have important implications for catalysis throughout the reaction cycle (Figure 4). Beginning with the (E-G) + S ground state, Narlikar *et al.* have proposed that docking of S to form the (E-S-G)<sub>C</sub> complex results in a destabilizing interaction with  $M_{\text{A}}$  because the electron-withdrawing phosphoryl group likely renders the 3'-oxygen electropositive relative to an oxygen from water.<sup>15</sup> Proceeding along the reaction coordinate, the  $M_{\text{A}}$  interaction becomes favorable in the transition state ((E-S-G)<sup>‡</sup>, Figure 4) due to the substantial negative charge that develops on the leaving group in phosphoryl transfer reactions.<sup>20</sup> The results herein show that when the 3'-atom bears a full negative charge,  $M_{\text{A}}$ -mediated substrate docking can provide approximately 3.6 kcal/mol of stabilization. A significant fraction of this stabilization likely occurs in the transition state, although the exact value may differ when  $\text{Mg}^{2+}$  and a leaving group oxygen are present instead of  $\text{Mn}^{2+}$  and sulfur. Following complete transfer of the phosphoryl group to form the (E-G<sub>p</sub>A-P<sub>O</sub><sup>-</sup>) complex, the immediate product of the ribozyme reaction,  $\text{P}_{\text{O}}^{-}$ , bears a full negative charge, and would experience further stabilization by the electrostatic environment. Subsequently,  $\text{P}_{\text{O}}^{-}$  becomes protonated to form  $\text{P}_{\text{OH}}$  in an energetically downhill reaction at neutral pH (Figure 4). In the reverse reaction (eq 1 and Figure 4), the electropositive character of  $M_{\text{A}}$  activates  $\text{P}_{\text{OH}}$  by increasing the amount of the more reactive  $\text{P}_{\text{O}}^{-}$  species, an effect expected to outweigh the decrease in reactivity due to metal ion coordination.<sup>3</sup>

Our results directly demonstrate that a metal ion has the capacity to impart catalysis through classic charge neutralization within a highly complex, active site environment, even one formed by a polyanionic RNA enzyme. The findings provide fundamental mechanistic insight into metallohydrolase function and metal-catalyzed phosphoryl transfer and represent an essential step toward quantitative accounting of metal ion catalysis of phosphoryl transfer by RNA and protein enzymes.

## METHODS

**RNA Synthesis.** L-21 *Scal Tetrahymena* ribozyme was prepared as described previously.<sup>21</sup> All oligonucleotides, unless otherwise noted, were purchased from Dharmacon (Lafayette, CO) and deprotected according to manufacturer's protocol. Details for the synthesis of  $\text{P}_{\text{H}}$  and  $\text{P}_{\text{SH}}$  as well as the steps taken to ensure the integrity of the -SH group are described in the Supporting Information. All RNA substrates were 5'-<sup>32</sup>P-end-labeled with [ $\gamma$ -<sup>32</sup>P]ATP (Perkin-Elmer) and T4 polynucleotide kinase (New England Biolabs), as previously described.<sup>21</sup>

**General Kinetics.** All reactions were carried out at 50 °C in 10 mM  $\text{MgCl}_2$  with the following buffers (50 mM): sodium acetate, pH 4.6–5.5; NaMES, pH 5.4–6.6; NaMOPS, 6.6–7.3; NaEPPS, 7.7–8.4 (pH values were determined at 50 °C). Details on the iodoacetamide modification assay, the miscleavage reaction, and pulse-chase experiments can be found in the Supporting Information.

## ASSOCIATED CONTENT

### Supporting Information

This material is available free of charge via the Internet at <http://pubs.acs.org>.

## AUTHOR INFORMATION

### Corresponding Author

\*E-mail: [herschla@stanford.edu](mailto:herschla@stanford.edu); [jpicciri@uchicago.edu](mailto:jpicciri@uchicago.edu).

## ACKNOWLEDGMENTS

This work was supported by grants from the National Institutes of Health to D.H. (GM 49243) and to JAP (AI081987). We thank A. Yoshida for initiating this work and providing the binding data shown in Table S1. We thank J. Lu and N.S. Li for oligonucleotide synthesis and M. Forconi, J. Schwans, and members of the Herschlag and Piccirilli laboratories for comments on the manuscript.

## REFERENCES

- Benkovic, S. J., & Schray, K. J. (1973) *Chemical Basis of Biological Phosphoryl Transfer* (Boyer, P. D., Ed.), pp 201–238, Academic Press, New York.
- Mitic, N., Smith, S. J., Neves, A., Guddat, L. W., Gahan, L. R., and Schenk, G. (2006) The catalytic mechanisms of binuclear metallohydrolases. *Chem. Rev.* 106, 3338–3363.
- Herschlag, D., and Jencks, W. P. (1990) Catalysis of the hydrolysis of phosphorylated pyridines by  $\text{Mg}(\text{OH})^+$ : a possible model for enzymatic phosphoryl transfer. *Biochemistry* 29, 5172–5179.
- Steitz, T. A., and Steitz, J. A. (1993) A general two-metal-ion mechanism for catalytic RNA. *Proc. Natl. Acad. Sci. U.S.A.* 90, 6498–6502.
- Hightower, K. E., Huang, C. C., Casey, P. J., and Fierke, C. A. (1998) H-Ras peptide and protein substrates bind protein farnesyltransferase as an ionized thiolate. *Biochemistry* 37, 15555–15562.
- Houglund, J., Piccirilli, J., Forconi, M., Lee, J., Herschlag, D. (2006) How the Group I Intron Works: A Case Study of RNA Structure and Function, In *RNA World*, 3rd ed. (Atkins, J. F., Gesteland, R. F., and Cech, T. R., Eds.), pp 133–205, Cold Spring Harbor Laboratory Press, Cold Spring Harbor, NY.
- Shan, S., Yoshida, A., Sun, S., Piccirilli, J. A., and Herschlag, D. (1999) Three metal ions at the active site of the *Tetrahymena* group I ribozyme. *Proc. Natl. Acad. Sci. U.S.A.* 96, 12299–12304.
- Stahley, M. R., and Strobel, S. A. (2005) Structural evidence for a two-metal-ion mechanism of group I intron splicing. *Science* 309, 1587–1590.
- Forconi, M., Lee, J., Lee, J. K., Piccirilli, J. A., and Herschlag, D. (2008) Functional identification of ligands for a catalytic metal ion in group I introns. *Biochemistry* 47, 6883–6894.

- (10) Oivanen, M., Kuusela, S., and Lonnberg, H. (1998) Kinetics and mechanisms for the cleavage and isomerization of the phosphodiester bonds of RNA by Bronsted acids and bases. *Chem. Rev.* 98, 961–990.
- (11) Herschlag, D. (1992) Evidence for processivity and two-step binding of the RNA substrate from studies of J1/2 mutants of the *Tetrahymena* ribozyme. *Biochemistry* 31, 1386–1399.
- (12) Narlikar, G. J., Bartley, L. E., Khosla, M., and Herschlag, D. (1999) Characterization of a local folding event of the *Tetrahymena* group I ribozyme: effects of oligonucleotide substrate length, pH, and temperature on the two substrate binding steps. *Biochemistry* 38, 14192–14204.
- (13) McConnell, T. S., Herschlag, D., and Cech, T. R. (1997) Effects of divalent metal ions on individual steps of the *Tetrahymena* ribozyme reaction. *Biochemistry* 36, 8293–8303.
- (14) Pecoraro, V. L., Hermes, J. D., and Cleland, W. W. (1984) Stability-Constants of  $Mg^{2+}$  and  $Cd^{2+}$  Complexes of adenine-nucleotides and thionucleotides and rate constants for formation and dissociation of MgATP and MgADP. *Biochemistry* 23, 5262–5271.
- (15) Narlikar, G. J., Gopalakrishnan, V., McConnell, T. S., Usman, N., and Herschlag, D. (1995) Use of binding energy by an RNA enzyme for catalysis by positioning and substrate destabilization. *Proc. Natl. Acad. Sci. U.S.A.* 92, 3668–3672.
- (16) Karbstein, K., Carroll, K. S., and Herschlag, D. (2002) Probing the *Tetrahymena* group I ribozyme reaction in both directions. *Biochemistry* 41, 11171–11183.
- (17) Jencks, W. P., Regenstein, J. (1979) *Ionisation Constants of Organic Acids in Aqueous Solution*, pp J187–J244, Pergamon Press, Oxford.
- (18) Weinstein, L. B., Earnshaw, D. J., Cosstick, R., and Cech, T. R. (1996) Synthesis and characterization of an RNA dinucleotide containing a 3'-S-phosphorothiolate linkage. *J. Am. Chem. Soc.* 118, 10341–10350.
- (19) Herschlag, D., Eckstein, F., and Cech, T. R. (1993) Contributions of 2'-hydroxyl groups of the RNA substrate to binding and catalysis by the *Tetrahymena* ribozyme. An energetic picture of an active site composed of RNA. *Biochemistry* 32, 8299–8311.
- (20) Lassila, J. K., Zalatan, J. G., and Herschlag, D. (2010) Biological phosphoryl-transfer reactions: understanding mechanism and catalysis. *Annu. Rev. Biochem.* 80, 699–702.
- (21) Zaug, A. J., Grosshans, C. A., and Cech, T. R. (1988) Sequence-specific endoribonuclease activity of the *Tetrahymena* ribozyme-enhanced cleavage of certain oligonucleotide substrates that form mismatched ribozyme substrate complexes. *Biochemistry* 27, 8924–8931.